RSC Advances

PAPER

View Article Online
View Journal | View Issue

Cite this: *RSC Adv.*, 2025, **15**, 22824

Increasing stiffness and thermal response behavior of collagen/metal nanoparticle composite hydrogels fabricated through radiochemical reduction†

Nazgul Assan, [a] Yuta Uetake, [ab] Tomoyuki Suezawa,[a] Rino Kamada,[a] Michiya Matsusaki, [a] Satoshi Seino[c] and Hidehiro Sakurai *[ab]

Received 14th May 2025
Accepted 26th June 2025

DOI: 10.1039/d5ra03384e

rsc.li/rsc-advances

Metal nanoparticle/hydrogel composites have attracted attention in the fields of materials science and applied chemistry. In this study, collagen/transition-metal nanoparticle (Col-TMNP) hydrogels are fabricated through radiochemical reduction on collagen-transition metal (Col-TM) gels, which we previously reported. ^{60}Co γ-ray irradiation of Col-Au and Col-Pt gels enables the uniform formation of metal nanoparticles within the collagen matrix, eliminating the need for chemical reducing agents. This method applies to a wide range of materials, regardless of their morphology or shape, and enables the synthesis of metal nanoparticles in a non-flowable gel state, which is difficult to achieve using solution-phase chemical reduction. The thus formed Col-AuNP and Col-PtNP gels exhibit enhanced elasticity compared to pristine Col-TM gels due to the formation of a cross-linking network structure by radiation-induced covalent bonds. Furthermore, the photothermal properties of Col-TMNP gels were examined using a Yb:YAG green laser (515 nm), showing a reversible photothermal response.

Introduction

Since the first report from Willner *et al.*,[1] the metal nanoparticle (NP)-hydrogel composites have attracted attention in the field of materials science and applied chemistry.[2–5] Loh *et al.* categorized five main approaches to obtaining uniformly dispersed NP-hydrogel composites; (1) hydrogel formation in a metal NP suspension, (2) physically embedding the metal NPs into hydrogel matrix after gelation, (3) reactive metal NP formation in a pre-formed gel, (4) cross-linking using metal NPs to form hydrogels, and (5) gel formation using NPs, polymers, and distinct gelator molecules. These methods are used for various purposes, leading to the development of a wide range of NP-hydrogel composites.[6]

Among various polymer matrices used as precursors for hydrogels, collagen has been extensively studied due to its outstanding biodegradability and biocompatibility.[7–14] Moreover, the hybridization of collagen with functional synthetic polymers can impart additional functionalities while preserving its inherent biological properties. Such hybrid materials have been widely employed in biomedical and materials science applications.[15–17] Among these functionalities, thermo-responsiveness is particularly attractive for drug delivery systems.[2] For instance, Chmielewski *et al.* reported collagen peptide–PEG-based hydrogels that exhibit temperature-sensitive behavior.[7]

In parallel, biopolymers such as collagen are often employed as stabilizing matrices for metal NPs, preventing their aggregation. The integration of metal NPs into polymer matrices not only improves their stability but also introduces novel physicochemical properties to the hydrogel system, thereby expanding its potential applications. In 2008, Slowinska *et al.* reported crosslinked collagen hydrogel functionalized with tiopronin-protected AuNPs through condensation reaction using 1-(3-dimethylaminopropyl)-3-ethylcarbodiimide (EDC).[8,9,13] These collagen/AuNP composites exhibited biodegradability and low cytotoxicity, as evaluated by CellTiter96 assays, suggesting their potential for applications in drug delivery, photothermal therapies, imaging, and cell targeting.[13] In addition to gold, collagen-transition metal composite, such as silver,[15,16] iron oxide,[17,18] Cr_2O_3,[19] Gd_2O_3,[20] La_2O_3,[21,22] Fe:Zn,[23] and so on,[24,25] have also been developed. Meanwhile, almost all preparation methods require pre-synthesized metal NPs with surfactant, which leads to the unavoidable chemical modification of

[a]*Division of Applied Chemistry, Graduate School of Engineering, The University of Osaka, 2-1 Yamadaoka, Suita, Osaka 565-0871, Japan. E-mail: hsakurai@chem.eng.osaka-u.ac.jp*

[b]*Innovative Catalysis Science Division, Institute for Open and Transdisciplinary Research Initiatives (ICS-OTRI), The University of Osaka, 2-1 Yamadaoka, Suita, Osaka 565-0871, Japan*

[c]*Management of Industry and Technology, Graduate School of Engineering, The University of Osaka, 2-1 Yamadaoka, Suita, Osaka 565-0871, Japan*

† Electronic supplementary information (ESI) available. See DOI: https://doi.org/10.1039/d5ra03384e

collagen chains and/or contamination with unnecessary chemicals.[26] A noteworthy exception is the method proposed by Jiao, Zou, and Yan *et al.*, which offers an alternative approach to forming collagen hydrogels containing AuNPs. This method involves electrostatic complexation between positively charged collagen chains and anionic Au species ($[AuCl_4]^-$), followed by a biomineralization sequence.[27,28] This method does not require pre-synthesis of metal NPs, allowing facile access to collagen-hydrogel composites.

In our previous study, we reported the rapid and specific gelation of collagen, triggered by the addition of transition-metal ions to afford collagen gels (Col-TM gel) (Scheme 1A).[29] Specifically, the introduction of a K_2PtCl_4 solution to a purified type I collagen solution in phosphate-buffered saline (PBS) resulted in gelation through the formation of a cross-linked network of collagen fibres with Pt(II) ions, yielding transparent and robust gels, Col-Pt. This discovery opens new avenues for applying collagen in transparent gelation within the biomedical field, particularly for 3D cultures of cells and organoids. Therefore, the collagen/transition-metal nanoparticle composite (Col-TMNP) gel, prepared from Col-TM gel, was expected to exhibit good physical properties with additional functionality specific to metal nanoparticles. In our case, however, the rapid gelation triggered by the addition of metal sources poses challenges for the preparation of Col-TMNP gels through conventional solution-phase reduction. Furthermore, the previously mentioned complexation/biomineralization method failed to produce metal NPs due to the weak reducing ability of collagen. To address this limitation, we recognized the need for a more general reduction method for metal NP formation that can proceed independently of the material's shape and form. Independent of this report, we also reported a process for preparing gold NPs *via* microchip laser (MCL) ablation of bulk gold, aiming to avoid metal-ion chelation. The MCL ablation method successfully produces gold NPs.[30] However, it still has limitations: the PBS buffer decomposes under ablation conditions, which leads to NP aggregation that we haven't yet been able to prevent.

In this context, we conceived of utilizing radiochemical reduction reactions. Since the initial discovery of the radiochemical synthesis of metal NPs, this method has been recognized as a clean and effective approach, as it eliminates the need for external chemical reducing agents.[31–34] It is also widely accepted that metal NPs produced through radiochemical methods exhibit uniform dispersion, as reduction and nucleation occur simultaneously.[35] Moreover, the use of high-energy radiation, such as γ-rays and electron beams, offers deep penetration, facilitating the scalability of the preparation process. Namely, we envisioned that the radiochemical reduction of metal ions in Col-TM gels induces nanoparticle formation to fabricate Col-TMNP gels. Herein, we report the preparation of Col-TMNP gels through the γ-ray irradiation method (Scheme 1B). In addition, the elasticity and thermal response of the thus prepared Col-TMNP gels were examined.

Experimental section

Materials

Pepsin-treated porcine skin type I and unpurified collagen sponges were donated by NH Foods Ltd, and the phosphate-buffered saline (PBS) solution of collagen nanofibers (CNFs) was prepared according to the literature procedure.[29] PBS powder was purchased from Sigma-Aldrich Japan Inc. and diluted with water (pH = 7.4). Acetic acid (CH_3CO_2H) was purchased from KISHIDA CHEMICAL Co., Ltd. Ethanol (99.5%) and silver nitrate ($AgNO_3 \cdot H_2O$) were purchased from Nacalai Tesque, Inc. Gelatin (077-03155), sodium chloride (NaCl), Tris–HCl buffer, dimethyl sulfoxide, acetone, *n*-hexane, tetrachloroaurate(III) trihydrate ($HAuCl_4 \cdot 3H_2O$), potassium tetrachloroplatinate(II) trihydrate ($K_2PtCl_4 \cdot 3H_2O$), copper(II) chloride ($CuCl_2 \cdot 2H_2O$), and nickel(II) chloride ($NiCl_2 \cdot 6H_2O$) were purchased from FUJIFILM Wako Pure Chemical Corp. Tetrahydrofuran (THF) and palladium(II) chloride ($PdCl_2$) were purchased from Kanto Chemical Co., Inc. Hexachloroplatinic(IV) acid hexahydrate ($H_2PtCl_6 \cdot 6H_2O$) was purchased by Tanaka Kikinzoku Kogyo Co., Ltd.

Preparation of Col-TMNP gels

0.2 wt% CNF in PBS solution (5 mL) was placed in a vial. To this was added aqueous metal ion solution (2.5 μmol) to afford Col-TM gel. The vial was sealed with a screw cap and exposed to ^{60}Co γ-ray irradiation at a commercial facility (Koga Isotope, Ltd) with the total absorbed dose was adjusted to approximately 20 kGy. The thus fabricated Col-TMNP gel was collected and subjected to further analysis. The shrinkage of the gel was evaluated by comparing the change in volume.

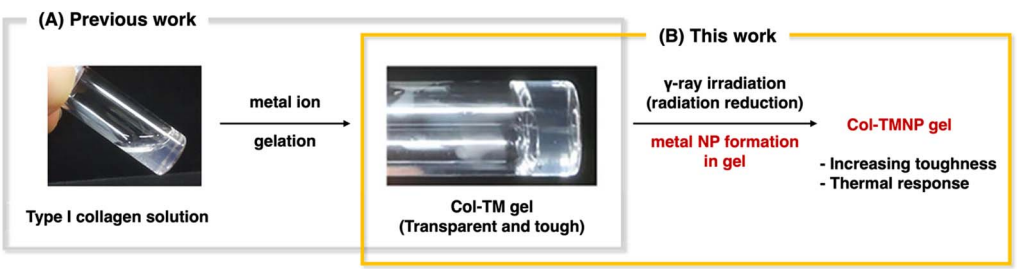

Scheme 1 γ-ray radiation induced metal nanoparticle formation in collagen gel. (A) Previous work. (B) This work.

Preparation of TEM sample for Col-TMNP gels

Transmission electron microscopy (TEM) observation was performed using a JEOL JEM-2100 electron microscope at an accelerating voltage of 200 kV. A holey carbon support film-coated copper microgrid (EM Japan, U1003) was applied with a hydrophilic treatment in a glow discharge irradiation chamber before use. Image-J software was used to analyse the TEM images, and the expressed mean diameter and standard deviation are based on an average of 300 particles. The Col-TMNP gel was placed on a glass slide and sliced into small pieces (1–5 mm) using a cutter. The trimmed Col-TMNP gel was carefully placed onto a pre-treated copper micro-grid and dried in a vacuum oven at 60 °C for 24 h. TEM observation was performed using the sample thus prepared.

Preparation of SEM sample for Col-TMNP gels

Scanning electron microscopy (SEM) images were recorded on a JEOL JSM-6701F field-emission scanning electron microscope at an accelerating voltage of 15 kV. The obtained images were analyzed using JEOL PC-SEM 6701 software. The hydrogels were lyophilized using a freeze-drying machine for 4 days. The dried samples were coated with a thin layer of osmium by an HPC-30 osmium coater before SEM observation. Then, SEM observation was performed using the sample thus prepared.

Compression test

Compression experiments were performed using a SHIMADZU EZ-Test or an Autograph AGS-20NX universal tensile instrument at room temperature. The moving speed and the maximum stress were set to 1 mm min^{-1} and 200 mN, respectively. A fabricated gel was hollowed out in cylindrical shape using a hole punch ($\varphi = 6$ mm) and trimmed to a certain height (3–8 mm). The exact initial diameter and height of the gel were measured using a digital calliper (CD-15CP, Mitsutoyo Corp.) three times, and the average values were used. The elastic modulus E (kPa) was calculated from the linear fitting of the stress–strain curve in the range between 5–10% strain (Fig. S4†).

Swelling ratio of collagen composite hydrogels

A Col-TMNP gel was freeze-dried for 24 hours, and the weight (W_{dry}) of the lyophilized gel was measured on a balance with a precision of ±0.1 g. Then, this was immersed in 2 mL PBS solution for 24 h, and the swollen sample was separated from the solution and placed on a glass. After soaking, the surface water was gently removed by filter paper, and the weight of the sample was determined on a balance (W_{wet}). Finally, the swelling ratios were calculated by the following equation:

$$\text{Swelling ratio (\%)} = (W_{wet} - W_{dry})/W_{dry} \times 100$$

This experiment was repeated four times, and the average value was expressed.

Photothermal activity

The temperature of the sample was monitored during the experiment using a K-type thermocouple connected to a digital thermometer (HD-1400K, Anritsu Corp.). The thermocouple was submerged in a Col-TMNP gel and placed near the laser axis. A Yb:YAG laser (515 nm, Spectra-Physics, MKS Instruments, Inc.) was positioned 25 cm from the sample, and the laser was irradiated onto the sample at a power of 50 mW for 5 min. After that, the laser was turned off, and the temperature was continuously monitored. This cycle was repeated twice, and the temperature was expressed as a mean value after three independent trials. The detail of the laser setup was shown in Fig. S5.†

Results and discussion

The Col-Au gel was prepared according to the previously reported procedure, using a 0.2 wt% CNF solution and an aqueous $HAuCl_4$ solution (2.5 μmol) (Fig. 1A). The thus prepared Col-Au gel was exposed to gamma radiation (^{60}Co) with a total absorbed dose of approximately 20 kGy. After irradiation, the color of the gel changed from almost colorless to reddish-brown, indicating the formation of metallic gold nanoparticles (AuNPs) exhibiting surface plasmon resonance. Notably, the gel state was maintained after irradiation, and the volume of the resulting Col-AuNP gel became 40% of that of the pre-irradiated Col-Au gel (Table 1). This suggested that the transition-metal-bridged intermolecular crosslinking of CNFs was retained, and the water contained in the CNF network structure was released. The obtained Col-AuNP gel was further analyzed by transmission electron microscopy (TEM), confirming the formation of AuNPs with a size of 4.1 ± 1.2 nm (Fig. 1B). Col-Au gel was also subjected to TEM observation, confirming no formation of AuNPs. Notably, γ-ray irradiation of the pristine Col solution also yielded a shrunken gel. However, non-transparent white gels were obtained. In addition, scanning electron microscopy (SEM) was performed on the Col-Au and Col-AuNP gels. SEM images of Col-Au gel showed an intricate morphology with an uneven surface (Fig. 1C). In contrast, that of Col-AuNP gel showed a more distinct separation of collagen fibers and reduced microstructural complexity (Fig. 1D). These morphological changes imply that γ-ray irradiation facilitates a degree of molecular reorganization within the collagen matrix, potentially affecting its mechanical properties.

Following the successful fabrication of Col-AuNP gel using the γ-ray irradiation method, we investigated the preparation of Col-TMNP gels with other metal sources, including platinum, palladium, silver, nickel, and copper. Col-Pt gels, which are known to form tough gels, were prepared using potassium tetrachloroplatinate (K_2PtCl_4) and hexachloroplatinic acid (H_2PtCl_6) and subjected to γ-ray irradiation under the same conditions (Col-Pt(II)NP and Col-Pt(IV)NP, respectively). After irradiation, brownish shrunken gels were formed while maintaining their gel texture. TEM analysis revealed that the formation of Col-PtNP with the particle sizes of 3.1 ± 1.6 nm and 3.4 ± 1.2 nm, respectively (Table 1, entries 2 and 3).

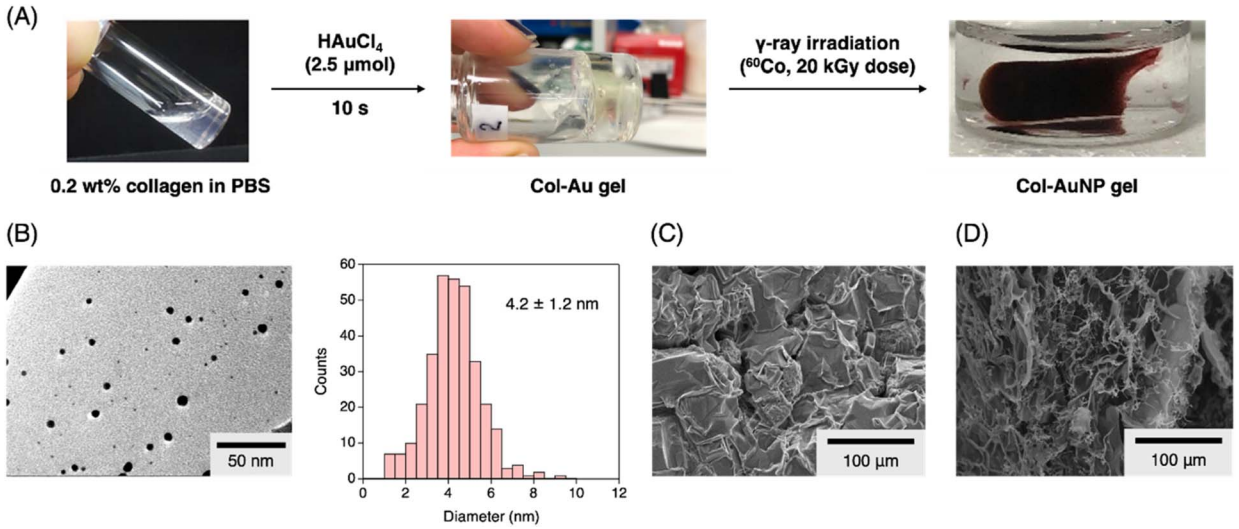

Fig. 1 Preparation of Col-AuNP gel. (A) Pictures for preparation. (B) TEM image and histogram. The mean diameter and standard deviation are based on the average for 300 particles. SEM images (C) before and (D) after γ-ray irradiation.

Table 1 Metal nanoparticle size of Col-TMNP gels[a]

Entry	Metal ion	Size[b] (nm)	Shrinkage (% v/v)
1	$HAuCl_4$	4.1 ± 1.2	40
2	K_2PtCl_4	3.1 ± 1.6	44
3	H_2PtCl_6	3.4 ± 1.2	36
4	$PdCl_2$	—	—
5	$AgNO_3$	—	—
6	$NiCl_2$	—	35
7	$CuCl_2$	—	21
8[a]	$HAuCl_4$	4.5 ± 1.5	25

[a] Mixture of type I and type III collagen was used. [b] The mean diameter and standard deviation are based on the average for 300 particles.

Although the Col-Pd gel was formed by mixing a Col solution and H_2PdCl_4, the Col-PdNP gels obtained became brittle after γ-ray irradiation and were not applicable for further measurements (entry 4). Meanwhile, Col-Ag gel was not obtained from the addition of silver nitrate ($AgNO_3$) due to the formation of silver chloride precipitates, which was ascribed to the remaining chloride in the PBS solution (entry 5). Col-Ni and Col-Cu gels prepared from nickel chloride ($NiCl_2$) and copper chloride ($CuCl_2$) were also examined, yielding non-transparent white gels, suggesting negligible formation of metal nanoparticles (entries 6 and 7). This would be attributed to the high redox potential of nickel and copper compared to that of noble metals. Col-TMNP gel formation proceeded successfully when a non-purified collagen (a mixture of Type I and Type III collagen) was used instead of the purified collagen. Col-AuNP gel with a particle size of 4.5 ± 1.5 nm was formed after irradiation when $HAuCl_4$ was used (entry 8). The use of gelatin, a component of a single collagen α-chain in the triple helix, did not afford gelled material before and after γ-ray irradiation.

Compression experiment

The elastic modulus of Col-TMNP gels was evaluated by compression tests. Fig. 2A and S4† represent the results of Col-TM and Col-TMNP gels. The elastic moduli of Col-Au, Col-Pt(II), and Col-Pt(IV) gels were 2.5, 3.1, and 1.9 kPa, respectively. Meanwhile, the elastic modulus of Col-AuNP was 10.1 kPa, which was five times higher than that of Col-Au gel. Similar trends were observed in the case of platinum. Col-Pt(II) and Col-Pt(IV) gels exhibited elastic moduli values of 5.8 and 16.9 kPa, respectively, which were also higher than those of the corresponding Col-Pt gels. To confirm the significance of these variations, we performed a statistical analysis using a two-tailed Student's *t*-test. Although the *p* value of Pt(II) gels was high ($p > 0.05$), those of Au(III) (0.074) and Pt(IV) (0.030) gel represent small *p* values around 0.05, showing the statistical significance in the case of Au(III) and Pt(IV) series. The increasing stiffness and shrinking of gels are probably attributed to the formation of covalent bonds that crosslink the network between collagen chains through radical reactions triggered by γ-ray irradiation. The schematic of the reaction mechanism for γ-ray reduction is summarized in Fig. 2D. Radiolysis of water produces reactive species, including reductive hydrated electrons (e_{aq}^-), hydrogen radicals ($H^\bullet$), and oxidative hydroxyl radicals ($HO^\bullet$). Given the high penetration capability of gamma rays, the generation of these reactive species occurs simultaneously and uniformly throughout the entire reaction field. Then, the thus formed reductive species (*e.g.*, e_{aq}^- and/or $H^\bullet$) react with metal ions to generate metal nanoparticles. Simultaneously, the hydrogen and hydroxy radicals also reacted with collagen chains to form radical species through the hydrogen abstraction reaction, which undergoes radical crosslinking and enhances their stiffness (Fig. 2E). Although the fate of the ionic species involved in the crosslinking in Col-TM gels is currently obscure, we assume that the metal–ligand coordination bonds in Col-TM gels were replaced by the covalent bonds as the reduction of metal ions

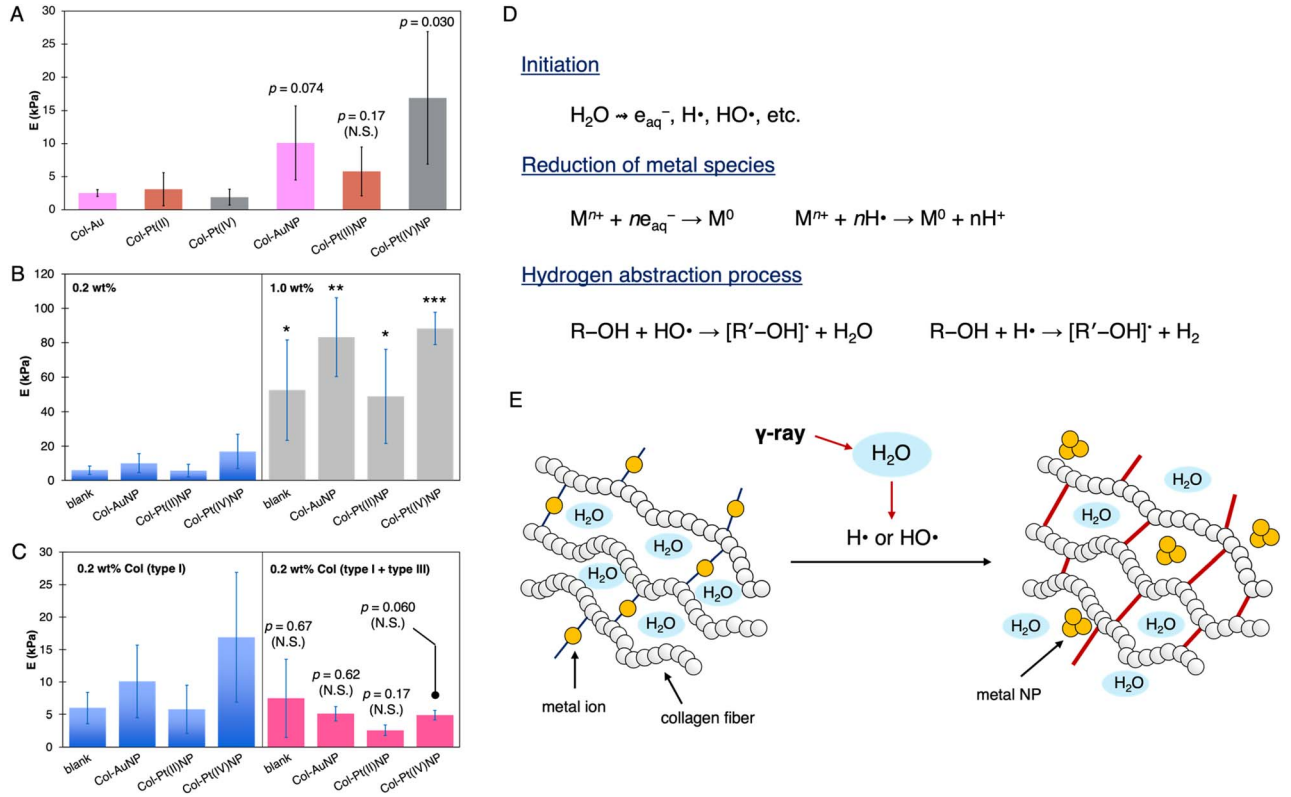

Fig. 2 Evaluation of elastic modulus of Col-TMNP gels and reaction mechanism. The values and standard deviations were calculated from four independent experiments ($n = 4$). Statistical analysis was performed using a two-tailed Student's t-test. *$p < 0.05$, **$p < 0.01$, ***$p < 0.001$. N.S. denotes no significance. (A) Comparison between Col-TM and Col-TMNP gels. The statistical analysis was relative to the corresponding Col-TM gels. (B) Effect of the collagen concentrations. The statistical analysis was relative to the corresponding 0.2 wt% Col-TMNP gels. (C) Effect of the collagen purity. (D) Schematics of the radiochemical reactions. (E) Schematic image of nanoparticle formation and radical crosslinking of collagen chains.

proceeds. The gel shrinkage would be caused by the covalent bonds that force collagen chains to be closer to each other. Given that the shape of the gels, other than size, has not changed, the metal ions in Col-TM gels is considered to act as a template. The stiffness was also investigated using a concentrated collagen solution. As expected, the elastic modulus of Col-TMNP gels increased in all cases and reached up to 88.3 kPa when Col-Pt(IV) gel was used as a precursor (Fig. 2B). The Student's t-test was also performed for the effect of collagen concentration, showing high significance ($p < 0.05$). Meanwhile, no significant variations were observed on the elastic modulus of Col-TMNP gels between purified and unpurified (mixture of type I and type III collagen) collagens (Fig. 2C).

Swelling ratio

To evaluate the water uptake ability, which affects the properties of hydrogels, such as thermal and mechanical stability as well as the mass transport ability, the swelling ratio of Col-TMNP gels was investigated. Lyophilized Col-TMNP gels were immersed in PBS solution for 24 h, and changes were observed. The swelling ratio of the irradiated Col gel was 430% (Table 2). Notably, no drastic difference was observed in the swelling ratio of Col-TMNP gels compared with that of Col gel. These results suggest that the morphology of Col-TMNP gels, particularly the pore size and intermolecular space within the cross-linked network structure, is primarily determined by the γ-ray irradiation step, rather than the transition metal cross-linking step. Meanwhile, collagen purity was found to have a significant impact on the swelling ratio, specifically in the case of Col-TMNP gels. Col-TMNP gels prepared with pure type I collagen exhibited significantly greater swelling ratios than the mixture of type I + III collagen. Although the reason is currently unclear, the results suggest that the Col-TMNP gels prepared from pure type I collagen exhibit a flexible morphology.

When compared with previously reported materials, the swelling ratios observed in this work is relatively high. For instance, Demeter *et al.*[36] reported swelling ratios slightly above

Table 2 Swelling ratio of collagen gels[a]

Gel	Type I (%)	Type I + III (%)	p
Col gel	430 ± 194	360 ± 59	0.464
Col-AuNP	540 ± 87	410 ± 53	0.070
Col-Pt(IV)NP	490 ± 78	690 ± 64	0.063

[a] The values and standard deviations were calculated from four independent experiments.

250% for collagen hydrogels crosslinked *via* electron beam irradiation, showing that stronger crosslinking often reduces water absorption. Similarly, Walimbe *et al.*[37] demonstrated substantially lower swelling (~35%) in hyaluronan-collagen hydrogels, attributed to the structural rigidity imparted by collagen. In contrast, the incorporation of nanoparticles in our Col-TMNP gels, particularly Pt(IV) NP, led to markedly higher swelling ratios, reaching up to 690%, which is in stark contrast to Fu *et al.*'s findings, where silver nanoparticles reduced swelling.[38] These comparisons suggest that while crosslinking methods and collagen type greatly influence hydrogel swelling, the incorporation of specific transition metal NPs can effectively enhance the swelling properties, likely by modifying the flexibility and water-holding capacity of the collagen network. Overall, these findings suggest that tailoring the type and interaction of embedded nanoparticles presents a promising approach for designing collagen-based hydrogels with customisable swelling properties for applications such as drug delivery, wound healing, and soft tissue engineering.

Photothermal activity of Au:Col and Pt:Col gels

To assess the practical applicability of the thus-prepared Col-TMNP gels, we conducted photothermal activity experiments. The γ-ray irradiated samples, Col-AuNP, Col-PtNP, and Col gels, were examined. Yb:YAG green laser (515 nm) was irradiated to the series of Col gels at room temperature, and the temperature fluctuations were monitored through the experiments. The laser power was set to 50 mW, and laser irradiation was continued for the initial 5 min. After that, the laser was turned off, and the temperature was continuously monitored for an additional 5 min. This cycle was repeated twice. The time course plots of the temperature fluctuations are shown in Fig. 3. The Col-AuNP gel exhibited a 6 °C temperature increase after 5 min. Meanwhile, the Col-PtNP exhibited a temperature increase of 3 °C, as PtNPs are a weaker absorber compared to AuNPs. Even the non-metal-containing Col-gels also showed a temperature increase of 1 °C, possibly due to localized heating. Notably, the same profiles were observed in the second cycles in all Col-gels, showing good stability under the laser irradiation conditions. These findings are consistent with previous studies on the photothermal properties of gold nanoparticles. For instance, Yang *et al.*[39] reported that SiO_2@Au core–shell nanoparticles exhibited temperature increases ranging from approximately 4 °C to 9.7 °C under 532 nm laser irradiation, depending on the morphology of the gold clusters on the silica core. The enhanced photothermal conversion in these NPs was attributed to strong near-field coupling and collective heating among gold clusters with uniform distribution. Similarly, Jaque *et al.*[40] discussed the efficiency of various nanoparticles for photothermal therapies, emphasizing the importance of NP composition and structure in determining photothermal performance. The observed temperature increases in the Col-AuNP gels align well with these studies, suggesting that the developed gels offer effective photothermal conversion, which is suitable for biomedical applications.

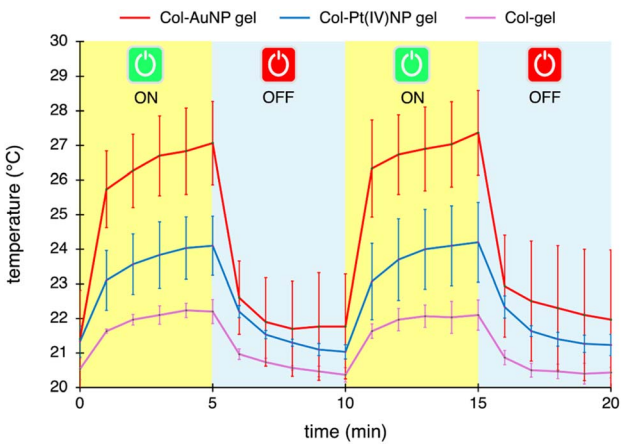

Fig. 3 Time course plots of temperature fluctuation under Yb:YAG green laser irradiation (515 nm). The error bars mean the standard deviations calculated from four independent experiments.

Conclusions

In conclusion, using the radiation reduction method, we have developed a practical preparation method for accessing collagen/metal nanoparticle (Col-TMNP) composite gels. Stiff collagen gels were successfully fabricated when transition-metal ions, such as Au and Pt, were used, and the elastic modulus increased to reach a maximum of 88 kPa after γ-ray irradiation. The impetus for this study was the failure of nanoparticle synthesis in collagen matrices by liquid-phase reduction, which was attributed to the unexpectedly rapid gelation of collagen induced by transition metal ions.[29] This issue has drawn our attention to the use of the radiation reduction method, which does not require chemical reducing agents and can be applied regardless of the substance's form. As a result, this study provides a facile and clean method for preparing Col-TMNP gels using γ-rays, which eliminates the need for chemical reducing agents. This study developed hydrogels with potential applications in both biomedical and environmental fields. Gel strength, elasticity, swelling behavior, and photothermal responsiveness were found to be influenced by both preparation conditions and the kind of loaded metal ions. γ-Ray irradiation not only promoted uniform nanoparticle formation but also induced covalent crosslinking of collagen chains, resulting in enhanced gel stiffness and a moderate decrease in swelling capacity. Further research into the application is in due course.

Data availability

All the data related to the manuscript are available in the ESI.†

Conflicts of interest

There are no conflicts to declare.

Acknowledgements

The authors are grateful to Dr Ryosuke Nishikubo (The University of Osaka) for helping with the photothermal activity

experiments. The authors are also grateful to Dr Masahiro Nakamoto (The University of Osaka) for helping with the compression experiments. This work was supported JSPS KAKENHI grant JP19K22187, JP24H00460 (H. S.); JP20K15279 (Y. U.); COI-NEXT (JPMJPF2009) from JST (M. M.); and JPNP20004 from NEDO (M. M.).

References

1 V. Pardo-Yissar, R. Gabai, A. N. Shipway, T. Bourenko and I. Willner, *Adv. Mater.*, 2001, **13**, 1320–1323.
2 P. Thoniyot, M. J. Tan, A. A. Karim, D. J. Young and X. J. Loh, *Adv. Sci.*, 2015, **2**, 1400010.
3 A. J. Clasky, J. D. Watchorn, P. Z. Chen and F. X. Gu, *Acta Biomater.*, 2021, **122**, 1–25.
4 G. D. Cha, W. H. Lee, C. Lim, M. K. Choi and D.-H. Kim, *Nanoscale*, 2020, **12**, 10456–10473.
5 J. H. Jeong, H.-C. Woo and M. H. Kim, *RSC Adv.*, 2021, **11**, 22826–22834.
6 O. Gazil, D. Alonso Cerrón-Infantes, N. Virgilio and M. M. Unterlass, *Nanoscale*, 2024, **16**, 17778–17792.
7 C. M. R. Pérez, L. A. Rank and J. Chmielewski, *Chem. Commun.*, 2014, **50**, 8174–8176.
8 L. Castaneda, J. Valle, N. Yang, S. Pluskat and K. Slowinska, *Biomacromolecules*, 2008, **9**, 3383–3388.
9 T. Schuetz, N. Richmond, M. E. Harmon, J. Schuetz, L. Castaneda and K. Slowinska, *Colloids Surf., B*, 2013, **101**, 118–125.
10 S. Poomrattanangoon and D. Pissuwan, *Heliyon*, 2024, **10**, e33302.
11 A. Arun, P. Malrautu, A. Laha, H. Luo and S. Ramakrishna, *Appl. Sci.*, 2021, **11**, 11369.
12 Q. K. Vo, A. T. Nguyen, H. T. Ho, L. T. N. Huynh, T. P. P. Nguyen and T. H.-T. Nguyen, *J. Nanomater.*, 2022, 4046389.
13 M. T. Aminzai and A. Patan, *J. Nanomater.*, 2024, 3280349.
14 A. C. Bîrcă, M. A. Minculescu, A.-G. Niculescu, A. M. Holban, A. Alberts and A. Mihai Grumezescu, *J. Funct. Biomater.*, 2025, **16**, 91.
15 H. Wu, L. He, M. Gao, S. Gao, X. Liao and B. Shi, *New J. Chem.*, 2011, **35**, 2902–2909.
16 A. Mandal, S. Sekar, N. Chandrasekaran, A. Mukherjee and T. P. Sastry, *J. Mater. Chem. B*, 2015, **3**, 3032–3043.
17 C. Alliraja, J. R. Rao and P. Thanikaivelan, *RSC Adv.*, 2015, **5**, 20939–20944.
18 A. Mandal, E. Dhineshkumar and E. Murugan, *ACS Omega*, 2023, **8**, 24256–24267.
19 S. Sangeetha, U. Ramamoorthy, K. J. Sreeram and B. U. Nair, *Colloids Surf., B*, 2012, **100**, 36–41.
20 V. Vijayan and M. S. Kiran, *Int. J. Biol. Macromol.*, 2023, **224**, 1423–1438.
21 V. Vijayan, R. Lakra, P. S. Korrapati and M. S. Kiran, *Colloids Surf., B*, 2022, **216**, 112589.
22 V. Vijayan, S. Sreekumar, K. M. Ahina, R. Lakra and M. S. Kiran, *Adv. Biol.*, 2023, **7**, 2300039.
23 K. V. Srivatsan, R. Lakra, K. Purna Sai and M. S. Kiran, *J. Mater. Chem. B*, 2016, **4**, 1437–1447.
24 M. Vedhanayagam, A. S. kumar, B. U. Nair and K. J. Sreeram, *Appl. Biochem. Biotechnol.*, 2022, **194**, 266–290.
25 S. Setoyama, R. Haraguchi, S. Aoki, Y. Oishi and T. Narita, *Int. J. Mol. Sci.*, 2024, **25**, 10439.
26 B. Pany, A. G. Majumdar, S. Bhat, S. Si, J. Yamanaka and P. S. Mohanty, *Heliyon*, 2024, **10**, e26244.
27 R. Xing, K. Liu, T. Jiao, N. Zhang, K. Ma, R. Zhang, Q. Zou, G. Ma and X. Yan, *Adv. Mater.*, 2016, **28**, 3669–3676.
28 H. Tohidi, N. Maleki and A. Simchi, *Int. J. Biol. Macromol.*, 2024, **280**, 135749.
29 T. Suezawa, N. Sasaki, Y. Yukawa, N. Assan, Y. Uetake, K. Onuma, R. Kamada, D. Tomioka, H. Sakurai, R. Katayama, M. Inoue and M. Matsusaki, *Sci. Adv.*, 2023, **10**, 2302637.
30 N. Assan, T. Suezawa, Y. Uetake, Y. Yakiyama, M. Matsusaki and H. Sakurai, *Colloids Interfaces*, 2025, **9**, 42.
31 J. Belloni, *Catal. Today*, 2006, **113**, 141–156.
32 Y. Yang, M. Johansson, A. Wiorek, N. V. Tarakina, F. Sayed, R. Mathieu, M. Jonsson and I. L. Soroka, *Dalton Trans.*, 2021, **50**, 376–383.
33 Y. Yang, G. Montserrat-Sisó, B. Wickman, P. A. Nikolaychuk and I. L. Soroka, *Dalton Trans.*, 2022, **51**, 3604–3615.
34 Y. Wang, M. Zhang, Z. Yan, S. Ji, S. Xiao and J. Gao, *Theranostics*, 2024, **14**, 1534–1560.
35 S. Seino, T. Kinoshita, T. Nakagawa, T. Kojima, R. Taniguci, S. Okuda and T. A. Yamamoto, *J. Nanopart. Res.*, 2008, **10**, 1071–1076.
36 M. Demeter, I. Călina, A. Scărișoreanu, M. Micutz and M. A. Kaya, *Materials*, 2022, **15**, 7663.
37 T. Walimbe, S. Calve, A. Panitch and M. P. Sivasankar, *Acta Biomater.*, 2019, **87**, 97–107.
38 H. Wu, L. He, M. Gao, S. Gao, X. Liao and B. Shi, *New J. Chem.*, 2011, **35**, 2902–2909.
39 L. Yang, Z. Yan, L. Yang, J. Yang, M. Jin, X. Xing, G. Zhou and L. Shui, *RSC Adv.*, 2020, **10**, 33119–33128.
40 D. Jaque, L. Martínez Maestro, B. Del Rosal, P. Haro-Gonzalez, A. Benayas, J. L. Plaza, E. Martín Rodríguez and J. García Solé, *Nanoscale*, 2014, **6**, 9494–9530.